SHEAR STRENGTHENING OF RC T-SECTION BEAMS WITH LOW STRENGTH CONCRETE USING NSM CFRP LAMINATES

S. J. E. Dias* and J. A. O. Barros

ISISE, University of Minho, Department of Civil Engineering, Azurém, 4810-058 Guimarães, Portugal

Abstract

The effectiveness of NSM technique with CFRP laminates for the shear strengthening of T-section RC beams of low strength concrete was assessed. Five NSM shear strengthening configurations (three CFRP orientations and two levels of CFRP percentage) were applied in RC beams with a steel stirrups percentage of 0.10% and of 0.17%. The results showed that: NSM technique is still effective in beams of low strength concrete; inclined are more effective than vertical laminates; the beam's shear resistance increases with the CFRP percentage; the NSM strengthening effectiveness decreases with the increase of the steel stirrups percentage. Using available experimental results obtained with the same test set-up but using beams of higher strength concrete it can be concluded that as minimum is the concrete strength as less effective is the NSM technique. In general, the formulation proposed by Nanni *et al.* provided safe and acceptable estimates for the contribution of the NSM shear strengthening systems (the predicted values of the CFRP contribution for the shear resistance were 75% of the results registered experimentally).

KEYWORDS: NSM, CFRP laminates, shear strengthening, T cross section RC beams, low strength concrete

1. Introduction

The use of Carbon Fiber Reinforced Polymer (CFRP) materials for structural repair and strengthening has continuously increased in the last years, due to several advantages resulting from opting for these composites in detriment of traditional construction materials such as steel, wood and concrete. These benefits include their high strength-to-weight ratio, high durability (non corrosive), electromagnetic neutrality, ease of handling, rapid execution with lower labor, and practically unlimited availability in size, geometry and dimension [1-3].

The shear failure mode of a Reinforced Concrete (RC) element should be avoided since it is brittle and unpredictable. For the shear strengthening, CFRP materials can be applied according to the followings two main

*Author to whom the correspondence should be sent (sdias@civil.uminho.pt).

techniques: bonding wet lay-up sheets or laminates to the external faces of the elements to be strengthened (Externally Bonded Reinforcement - EBR - technique) [4-7]; installing CFRP bars (circular, square or rectangular cross section) into pre-cut slits opened on the concrete cover of the elements to strengthen (Near Surface Mounted - NSM - technique) [8-11]. Due to the largest bond area and higher confinement provided by the surrounding concrete, narrow strips of CFRP laminates of rectangular cross section, installed into thin slits and bonded to concrete by an epoxy adhesive, are the most effective CFRP strengthening elements for the NSM technique [12]. Dias and Barros demonstrated by experimental research that NSM technique provides higher effectiveness than EBR technique for the shear strengthening of rectangular cross sectional RC beams without steel stirrups [13] and T cross sectional RC beams having a certain percentage of existing steel stirrups [14].

There are several reasons that justify the relevance of a study on the use of the NSM technique with CFRP laminates for the shear strengthening of RC beams of low strength concrete: old RC structures were built with low strength concrete; decrease of concrete strength due to several time dependent phenomena and environmental conditions; experimental results of shear strengthening of RC beams using NSM technique with CFRP laminates indicate that concrete has an important role in the effectiveness of this technique [14-15]. This last experimental evidence was also obtained with a recent analytical/numerical model that involves the kinematic conditions of the shear crack propagation in a NSM shear strengthened RC beam, as well as the concrete fracture and laminate-adhesive-concrete bond main characteristics [16].

To appraise the possibility of the application of NSM CFRP laminates for the shear strengthening of T cross sectional reinforced low strength concrete beams having a certain percentage of existing steel stirrups, an experimental program was carried out. The average value of the concrete compressive strength at age of the beams tests was 18.6 MPa. The experimental program is outlined and the specimens, materials and test set-up are described. The results of the tests are presented and discussed and a number of conclusions are drawn. Taking the results obtained in a previous experimental program [14-15], characterized by the same test set-up but using beams of higher concrete strength (39.7 MPa instead of 18.6 MPa), the influence of the concrete mechanical properties in the performance of the NSM technique with CFRP laminates for the shear strengthening of RC beams was assessed.

Additionally, the predictive performance of the formulation proposed by Nanni *et al.* [11] for the NSM shear strengthening technique was appraised taking the results obtained in the present experimental program.

2. Experimental program

2.1 Beam prototypes

Fig. 1 presents the T cross section of the thirteen beams comprising the experimental program. The reinforcement systems were designed to assure shear failure for all the tested beams. To localize the shear failure in one only of the beam shear spans, a three point load configuration of distinct length of the beam shear spans was selected, as shown in Fig. 1. The monitored beam span (L_i) is 2.5 times the effective depth of the beam cross section ($L_i/d=2.5$), since, according to the available research [17], this is the minimum value with negligible arch effect. To avoid shear failure in the L_r span, steel stirrups ϕ6@75mm were applied in this span. The differences between the tested beams are restricted to the shear reinforcement systems applied in the L_i beam span.

The experimental program is made up of three reference beams and two groups of NSM shear-strengthened beams. The reference beams comprehend (see Fig. 1 and Fig. 2): one beam without any shear reinforcement (C-R beam); one beam with steel stirrups ϕ6@300mm (2S-R beam, with a percentage of stirrups, ρ_{sw}, of 0.10%); one beam with steel stirrups ϕ6@180mm (4S-R beam, with a percentage of stirrups, ρ_{sw}, of 0.17%). For the NSM shear-strengthened beams, the first group is composed by five beams (2S-7LV, 2S-4LI45, 2S-7LI45, 2S-4LI60 and 2S-6LI60) presenting the percentage of stirrups as adopted in the 2S-R reference beam (ρ_{sw} = 0.10%), and having the CFRP shear strengthening arrangements indicated in Table 1 and Fig. 2. The second group also comprehends five beams (4S-7LV, 4S-4LI45, 4S-7LI45, 4S-4LI60 and 4S-6LI60), having the percentage of stirrups used in the 4S-R reference beam (ρ_{sw} = 0.17%), and the adopted strengthening configurations were the same applied in the first group of beams (see Table 1 and Fig. 2). Three CFRP orientations (45º, 60º and 90º) were tested, and for inclined laminates two CFRP percentages were adopted. For the both two groups the beams with the lower percentage of laminates were designed in order to present similar maximum load, regardless of the orientation of the laminates [14]. The same strategy was adopted on the design of the beams strengthened with the higher percentage of laminates. Moreover, the two groups of beams were also conceived to study the influence of the amount of existing steel stirrups on the effectiveness of the NSM shear strengthening technique.

According Fig. 1, the laminates were distributed along the AB line, where A represents beam support at its “test side” and B is obtained assuming a load degradation at 45º.

The three point beam bending tests (Fig. 1) were carried out using a servo closed-loop control equipment, taking the signal read in the displacement transducer (LVDT), placed at the loaded section, to control the test at a deflection rate of 0.01 mm/second. To prevent brittle spalling of the concrete cover at the supports, the beam ends were strengthened by confining the concrete with a two-directional cage of ϕ6@65mm horizontal stirrups and ϕ12@50mm vertical stirrups ϕ6 mm (Fig. 1). To overcome the difficulties to bend ϕ32 mm longitudinal tensile bars, their ends were welded to steel plates.

With the purpose of obtaining the strain variation along the two laminates that have the highest probability of providing the largest contribution for the shear strengthening of the RC beam, four strain gauges (SG_L) were bonded in each CFRP according to the arrangement represented in Fig. 3. Adopting the same principle, one steel stirrup was monitored with three strain gauges (SG_S) installed according to the configuration represented in Fig. 3. The location of the monitored laminates and stirrups in the tested beams is represented in Fig. 2.

2.2 Material properties

The concrete compressive strength was evaluated at 28 days and at the age of the beam tests, carrying out direct compression tests with cylinders of 150 mm diameter and 300 mm height, according to EN 206-1 [18]. In the tested beams, high bond steel bars of 6, 12, 16 and 32 mm diameter were used. The values of their main tensile properties were obtained from uniaxial tensile tests performed according to the recommendations of EN 10002-1 [19]. The tensile properties of the CFK 150/2000 S&P laminates, with a cross section area of 1.4×9.5 mm^2, were characterized by uniaxial tensile tests carried out according to ISO 527-5 [20]. Table 2 includes the average values obtained from these experimental programs. The MBrace Resin 220 [21] epoxy adhesive was used to bond the laminates to the concrete.

2.3 Strengthening technique

To apply the precured CFRP laminates using NSM technique, the following procedures were executed: 1) using a diamond cutter, slits of about 4-5 mm width and 12-15 mm depth were opened on the concrete cover (of about 22 mm thickness) of the lateral faces of the beam web, according to the pre-defined arrangement for the laminates (the laminates were not anchored to the beam flange; they were restricted to the beam web); 2) the slits were cleaned by compressed air; 3) the laminates were cut with the desirable length and cleaned with acetone; 4) the epoxy adhesive was produced according to the supplier recommendations; 5) the slits were filled with the adhesive; 6) a layer of adhesive was applied on the faces of the laminates; and 7) the laminates were inserted into the slits and adhesive in excess was removed.

To guarantee a proper curing of the adhesive, at least one week passed between the beam strengthening operations and the beam test.

3. Results

3.1 Load carrying capacity of the tested beams

The relationship between the applied force and the deflection at the loaded section (u_{LS}) for the tested beams is represented in left part of Fig. 4 and Fig. 5, respectively, for the lower and higher percentage of steel stirrups. As Fig. 4b shows, ΔF represents the increase of the load provided by a shear strengthening system, while F^{ref} is the corresponding load capacity of the reference beam. For deflections greater than the corresponding to the formation of the first shear crack in the reference beam, the $\Delta F / F^{ref}$ ratio was evaluated, and the $\Delta F / F^{ref}$ *vs* u_{LS} relationship is depicted in the right part of Fig. 4 (the reference beam is 2S-R) and Fig. 5 (the reference beam is 4S-R). For the tested beams, the $\left(\Delta F / F^{ref}\right)_{max}$ value and the corresponding deflection at the loaded section, $u_{\left(\Delta F / F^{2S-R}\right)_{\max}}$, are indicated in Table 3. Assuming that F_{max} and F_{max}^{ref} are the load carrying capacities (maximum force) of strengthened and reference beams (2S-R or 4S-R) the values of $\Delta F_{max} / F_{max}^{ref}$ were evaluated ($\Delta F_{max} = F_{max} - F_{max}^{ref}$). These values and the deflection at loaded section associated to F_{max} ($u_{F_{max}}$) are included in Table 3.

Fig. 4 and Fig. 5 and the results included in Table 3 show that, for deflections higher than the one corresponding to the formation of the first shear crack in the reference beams (u_{LS} = 1.29 mm for 2S-R (Fig. 4) and u_{LS} = 1.26 mm for 4S-R (Fig. 5)), the adopted CFRP configurations provided an increase in the beam's load carrying capacity. This reveals that the CFRP laminates bridging the surfaces of the shear crack offer resistance, mainly, to crack opening, resulting a smaller degradation of the shear stress transfer between the faces of the crack due to aggregate interlock effect. Therefore, for deflections above the deflection corresponding to the formation of the shear crack in the reference beams, an increase of the beam's stiffness is observed in the shear strengthened beams. The crack opening resisting mechanisms provided by the crack bridging laminates also contribute to increase the load at which stirrups enter in their plastic phase.

The strengthening arrangements with the lower percentage of CFRP (only beams with inclined laminates) had the following increments in terms of beam load carrying capacity ($\Delta F_{max} / F_{max}^{ref}$): 24.9% and 24.3% for the beams strengthened with laminates at 45º (2S-4LI45 beam) and laminates at 60º (2S-4LI60 beam), respectively, for the beams with two steel stirrups in the smaller beam shear span; 14.3% and 13.8% for the beams strengthened with laminates at 45º (4S-4LI45 beam) and laminates at 60º (4S-4LI60 beam), respectively, for the beams with four steel stirrups in the smaller beam shear span. In terms of $\left(\Delta F / F^{ref}\right)_{max}$, only the beams with laminates at 60º presented higher value than the one obtained for $\Delta F_{max} / F_{max}^{ref}$ (27.4% for 2S-4LI60 beam and 19.6% for 4S-4LI60). Laminates at 45º and 60º had similar performance in terms of maximum load. The beams with laminates at 60º had better performance than the beams with laminates at 45º in terms of stiffness.

For the beams shear strengthened with the higher CFRP percentage, the strengthening configurations with inclined laminates were more effective than CFRP arrangement at 90º. Vertical laminates, laminates at 45º and laminates at 60º assured an increase of $\Delta F_{max} / F_{max}^{ref}$: 20.8%, 35.3% and 31.4%, respectively, for the beams with two steel stirrups in the smaller beam shear span; and 3.8%, 17.3% and 19.3%, respectively, for the beams with four steel stirrups in the smaller beam shear span. For the higher percentage of the CFRP the values of $\left(\Delta F / F^{2S\text{-}R}\right)_{max}$ of the beams 2S-7LV (26.1%), 2S-7LI45 (38.5%), 4S-7LV (6.7%), 4S-7LI45 (19.3%) and 4S-6LI60 (20.9%) were higher than the values of $\Delta F_{max} / F_{max}^{ref}$. For the arrangements with laminates at 45º and 60º the values of $\left(\Delta F / F^{ref}\right)_{max}$ and $\Delta F_{max} / F_{max}^{ref}$ increased with the percentage of CFRP.

The comparison between Fig. 4 and 5 and the results included in Table 3 show that the amount of existing steel stirrups plays a very important role on the effectiveness of the NSM shear strengthening technique. In fact, the effectiveness of the CFRP was higher in the beams with the lower percentage of steel stirrups analyzed. According to the experimental results, for an increase from 0.1% to 0.17% in the percentage of steel stirrups in the L_i beam span, the NSM strengthening effectiveness decreased in about 55% (see Fig. 6 - the value regarding the configuration with vertical laminates was excluded). For the solutions with inclined laminates, the average value of $\Delta F_{max} / F_{max}^{ref}$ varies from 29.0% to 16.2% when the amount of stirrups changes from ϕ6@300 mm (ρ_{sw} = 0.10%) to ϕ6@180 mm (ρ_{sw} = 0.17%), meaning that the interaction with stirrups plays a detrimental effect on the effectiveness of the NSM strengthening system. This fact was also observed by Dias and Barros [15] when the five NSM arrangements adopted in the present experimental program were applied in identical beams with a concrete of higher compressive strength (in this case for an increase from 0.1% to 0.17% in the percentage of steel stirrups in the L_i beam span, the NSM strengthening effectiveness decreased in about 70% - see section 4). This is an important aspect due to the fact that existing RC beams requiring shear strengthening intervention often have a certain percentage of steel stirrups. It emerges that a formulation for the prediction of the NSM shear strengthening contribution cannot neglect the percentage of existing steel stirrups.

3.2 Failure modes

As was expected, all the tested beams failed in shear (Fig. 7). In this figure, the steel stirrups of the smaller beam shear span are indicated by vertical lines, and the circles indicate the zone where stirrups have ruptured.

When the maximum load of the C-R beam was attained the shear failure crack widen abruptly. The maximum load of the 2S-R and 4S-R beams was attained when one stirrup crossing the shear failure crack has ruptured.

In the NSM beams strengthened with the lowest percentage of CFRP the laminates failed by "debonding". However, in the present context "debonding" should not be assumed as a pure debonding failure mode of the laminate, since along its bond length, parts of concrete were adhered to the laminate, indicating that failure includes debond and concrete fracture, which is in agreement with the principles of the model of Bianco *et al.* [16]. In the beams with the highest percentage of CFRP a group effect takes place and the concrete cover delamination (premature detachment of a concrete layer that includes the laminates) is found to be the critical failure mode. This indicates that the efficacy of NSM shear strengthening might be limited by laminate spacing. Fig. 8 clarifies the influence of CFRP percentage in the failure modes of the beams.

The global analysis of failure modes of the tested beams with CFRP indicates that the efficacy of NSM technique for the shear strengthening of RC beams using CFRP laminates is dependent of the concrete strength and increases with the quality of this material. In section 4 of the present paper is possible to verify this evidence by experimental results.

3.3 Strains in the CFRP and steel stirrups

The maximum strain recorded in the laminates up to the maximum load of the beams (ε_{CFRP}^{max} - see Table 3) ranged from 0.54% (beam 4S-6LI60) and 0.94% (beam 2S-4LI45). In terms of the average strain of the maximum strain values registered in the monitored laminates (two per beam) (($\varepsilon_{CFRP}^{max})_{med}$ - see Table 3), the variation was between 0.41% in the 4S-7LV and 0.88% in the 4S-4LI45. For all the tested NSM beams the average value of ε_{CFRP}^{max} and ($\varepsilon_{CFRP}^{max})_{med}$ was 0.72% and 0.62%, respectively. In terms of CFRP orientation, the average value of the maximum strain (ε_{CFRP}^{max}) was 0.81%, 0.67% and 0.64% for the beams with laminates at 45º, 60º and 90º, respectively. These values ranged from 39% to 50% of the CFRP ultimate rupture strain (ε_{fu} = 1.63% - see Table 2).

To illustrate a representative strain variation in monitored laminates and stirrup during the beam loading process, the strain values for distinct load levels of the 4S-4LI45 beam are indicated in Table 4, from which it can be observed that the maximum strain value was 0.84‰ (SG_L2 and SG_L3) in the CFRP A and 0.93‰ (SG_L2) in the CFRP B. The strain values of the monitored stirrup of the 4S-4LI45 and 4S-R beams for four loads levels, included in Table 4 (the values of the 4S-R beam are in the round brackets), show that the steel stirrup was more strained in the reference beam than in the strengthened beam. The CFRP laminates bridging the faces of the shear failure crack offer some resistance to the crack opening. This mechanism also decreases the loss of the concrete aggregate interlock contribution for the shear resistance that occurs with the crack opening of the shear failure crack. Due to these effects, the strains on the steel stirrups of the CFRP strengthened beams were lower than the strains recorded in the reference beam, at equal load levels applied to the beams.

Fig. 9 represents the variation of the strains on the monitored laminates (see Table 4) during the loading process up to the maximum load of the 4S-4LI45 beam. It is observed that the curves feature two phases. In the initial stage of loading, the CFRP did not contribute to the load-carrying capacity of the beam. In the second stage, the laminate began to strain due the formation of a crack that crossed the laminate. The strain in the laminate continued to increase with the increase of the load up to the maximum force of the beam (the exception was the SG_L1 in the CFRP A). Fig. 9 evidences that both laminates were crossed by more than one crack. In the CFRP A, SG_L2 and SG_L3 were closer to the shear crack zone than the other strain gauges, while in the CFRP B this happened to the SG_L2. Therefore the strain variation depends significantly on the relative position between SGs and the formed cracks. Fig. 10 represents the variation of the strains on the monitored stirrup during the loading process up to the maximum load of the 4S-4LI45 beam, being possible to observe the presence of the same two phases already identified in laminates. In the last phase of the strain variation in the steel stirrup of the 4S-4LI45 beam the strain registered in SG_S decreased with the increase of the load. This was caused by the formation of the shear failure crack that did not cross this steel stirrup (Fig. 7).

4. Influence of the concrete strength on the effectiveness of the NSM technique

In the present section the influence of concrete strength on the efficacy of the NSM technique is assessed comparing the results of the experimental program described in previous sections with the results of other experimental program [14, 15] dealing with beams of higher concrete strength. In this experimental program the five arrangements of NSM CFRP laminates presented in Fig. 2 were also used but the beams were manufactured with a concrete of a compressive strength at the age of beam tests of 39.7 MPa (f_{cm} = 39.7 MPa instead of f_{cm} = 18.6 MPa - see Table 2). The remaining characteristics were the same in both experimental programs.

The values of the $\Delta F_{max}/F_{max}^{ref}$ ratio, $u_{F_{max}}/u_{F_{max}}^{ref}$ ratio ($u_{F_{max}}^{ref}$ is the the deflection at loaded section corresponding to F_{max}^{ref}) and the maximum strain recorded in the laminates (ε_{CFRP}^{max}) for the beams of the above mentioned experimental programs are included in Table 5. The $\Delta F_{max}/F_{max}^{ref}$ ratio is also represented in Fig. 11, being visible the increase of the NSM effectiveness with the increase of the concrete strength. According to the values into Table 5, the average value of the $\Delta F_{max}/F_{max}^{ref}$ ratio for NSM arrangements adopted in beams with higher and lower concrete compressive strength was 26.5% and 22.4%, respectively (the values regarding the 4S-4LV shear strengthening configuration was excluded for this analysis). The better performance of the CFRP when applied in the beams with f_{cm} = 39.7 MPa was also observed in terms of the $u_{F_{max}}/u_{F_{max}}^{ref}$ ratio. The average value of the $u_{F_{max}}/u_{F_{max}}^{ref}$ ratio for NSM arrangements adopted in beams with higher and lower concrete compressive strength was 22.7% and 6.9%, respectively (the values regarding the 4S-4LV shear strengthening configuration was excluded for this analysis). Furthermore, in the group of beams of higher concrete strength larger maximum strain values were registered, which indicates that the laminates are more effectively mobilized as higher is the strength of the concrete. The average value of the maximum strain recorded in the laminates up to the maximum load of the beams (ε_{CFRP}^{max}) was 0.9% for beams with f_{cm} = 39.7 MPa and 0.72% for beams with f_{cm} = 18.6 MPa.

The ~~typical~~ failure modes obtained in the ~~series of~~NSM beams of ~~distinct concrete strength class are characterized by i) the fracture of a concrete volume surrounding the bond length of the CFRP laminate; ii) a mix mode composed of concrete fracture followed by debond. In fact, after failure, a certain volume of concrete is bonded to the CFRP laminate, and the propensity for the occurrence of the failure mode i) seems to be as high as lower is the concrete strength class, as proved by Bianco et al. [16]~~the both experimental programs were similar (see section 3.2). However, due the higher concrete strength, the decrease of the effective bond length, in consequence of the fracture failure of concrete surrounding a laminate crossing the critical diagonal crack, was not so pronounced as occurred in the beams of lower concrete strength class. ~~. In this case, the tensile strength of the concrete surrounding the CFRP bond length is the main governing parameter of the NSM shear strengthening effectiveness. For beams of concrete of higher strength class, concrete fracture is, in general, the first failure occurrence, leading to a reduction of the effective bond length of the CFRP, thereby the aforementioned mix mode is the typical failure mechanism.~~ In consequence, the higher is the tensile strength of the concrete surrounding the laminates, the larger is the contribution of the NSM CFRP laminates for the shear resistance of RC beams.

5. Comparison of experimental and analytical results

Taking the results obtained in the tested beams strengthened with NSM technique, the predictive performance of the analytical formulation proposed by Nanni *et al.* [11] was appraised. According this formulation, the term within the square brackets of the equation (1) is the force resulting from the tensile stress in the NSM FRP elements crossing the shear failure crack. The vertical projection of this force is the contribution of the FRP to the shear resistance of the beam (V_f),

$$V_f = \left[4 \cdot \left(a_f + b_f\right) \cdot \tau_b \cdot L_{tot\,min}\right] \cdot sin\,\theta_f \tag{1}$$

being τ_b the average bond stress of the FRP elements intercepted by the shear failure crack, and $L_{tot\ min}$ is obtained from (see Fig. 12),

$$L_{tot\,min} = \sum_i L_i \tag{2}$$

where L_i represents the length of each single NSM laminate intercepted by a 45-degree shear crack, determined from,

$$L_i = \begin{cases} min\left(\dfrac{s_f}{cos\,\theta_f + sin\,\theta_f} i;\ l_{max}\right) & i = 1.....\dfrac{N}{2} \\ min\left(l_{net} - \dfrac{s_f}{cos\,\theta_f + sin\,\theta_f} i;\ l_{max}\right) & i = \dfrac{N}{2} + 1.....N \end{cases} \tag{3}$$

$L_{tot\ min}$ corresponds to an arrangement of the FRP reinforcements crossing the shear failure crack that leads to the minimum of the $\sum_i L_i$. In (3) l_{net} is defined as,

$$l_{net} = l_b - \frac{2c}{sin\,\theta_f} \tag{4}$$

which represents the net length of a FRP laminate, as shown in Fig. 12, to account for cracking of the concrete cover and installation tolerances. In (4), l_b is the actual length of a FRP laminate and c is the concrete clear cover thickness.

The first limitation of (3) takes into account bond as the controlling failure mechanism, and represents the minimum effective length of a FRP laminate intercepted by a shear crack as a function of the term *N*,

$$N = \frac{l_{eff}\left(1 + cot\,\theta_f\right)}{s_f} \tag{5}$$

where N is rounded off to the lowest integer (e.g., N=5.7 $\Rightarrow$ N = 5), and l_{eff} represents the length of the vertical projection of l_{net} as shown in Fig. 12,

$$l_{eff} = l_b \sin\theta_f - 2c \tag{6}$$

The second limitation in (3), $L_i = l_{max}$, results from the force equilibrium condition, taking an upper bound value for the effective strain, ε_{fe} (see Fig. 13),

$$l_{max} = \frac{\varepsilon_{fe}}{2} \cdot \frac{a_f \cdot b_f}{a_f + b_f} \cdot \frac{E_f}{\tau_b} \tag{7}$$

The design contribution of the NSM laminates to the shear resistance of the beams is defined as,

$$V_{fd} = \phi\ \psi_f\ V_f \tag{8}$$

being ϕ the strength-reduction factor indicated by ACI [22] that, for shear strengthening of concrete elements has a value of 0.85. For the additional reduction factor ψ_f, the value of 0.85 recommended by ACI [1] for EBR technique (bonded face schemes) was adopted.

Adopting for ε_{fe} and τ_b the values recommended by Barros and Dias [13], respectively, 0.59% and 16.1 MPa, assuming for the elastic modulus of the laminate the average value recorded in the experimental program of the present work (174.3 GPa), the values of the contribution of the NSM laminates for the shear strengthening of the tested beams (V_{fd}^{ana}), included in Table 6, are compared to those registered experimentally ($V_f^{exp.}$). These values were obtained by subtracting the shear resistance of the reference beam (2S-R beam or 4S-R beam) from the shear resistance of the NSM strengthened beam. Apart the too abnormal low contribution of the laminates registered in the tested 4S-7LV beam, the values of $V_f^{exp.} / V_{fd}^{ana.}$ are very closer or higher than one (safety condition), and decrease with the increase of the CFRP percentage. An average value of about 1.47 for $V_f^{exp.} / V_{fd}^{ana.}$ was obtained. Regarding the influence of the percentage of steel stirrups, the average value of $V_f^{exp.} / V_{fd}^{ana.}$ was 1.59 and 1.32 for beams with ρ_{sw} equal to 0.10% and 0.17%, respectively. This difference can be justified by the fact the analytical formulation proposed by Nanni *et al.* [11] does not consider the detrimental effect of the influence of the percentage of transverse steel stirrups in the contribution of the NSM laminates.

6. Conclusions

The effectiveness of the NSM technique for the shear strengthening of T cross section RC beams of low concrete strength was analysed by carrying out an experimental program. This effectiveness was appraised by assessing the contribution provided by the distinct CFRP shear strengthening arrangements in terms of load carrying capacity, stiffness of the response of the beams after the formation of the shear failure crack in the reference beam, maximum strains measured in the CFRP laminates, and failure modes. The influence of the percentage and inclination of the laminates and the percentage of existing steel stirrups was also evaluated.

From the obtained results it can be concluded that the shear strengthening technique is still effective in RC beams of an average concrete compressive strength of 18.6 MPa at the age of the beams tests, which can be considered as the lowest concrete strength class for structural purposes. The CFRP shear strengthening configurations provided an increase not only in terms of maximum load, but also in terms of load carrying capacity after shear crack formation. The concrete strength has, however, an important role on the effectiveness of the NSM shear strengthening technique, since this effectiveness decreases with the decrease of the concrete strength. In fact, when the same NSM CFRP laminates arrangements were applied in a group of beams of concrete compressive strength (f_{cm}) equal to 39.7 MPa and in another group of beams of f_{cm}=18.6 MPa, the CFRP laminates were more effective in the former beams. In the beams of lower concrete strength class a predominant fracture of concrete surrounding the bond length of the laminates has occurred, while in the series of beams of larger concrete strength class a mix mode composed by concrete fracture followed by debond was the typical failure mode. The mix mode is generally associated to a higher effectiveness of the NSM CFRP laminates for the shear resistance of RC beams than the concrete fracture.

Inclined laminates were more effective than vertical laminates and an increase of the percentage of laminates led to an increase of the shear capacity of the beams. A detrimental effect of the increase of the percentage of the existing steel stirrups exists in terms of the effectiveness of the NSM technique for the shear resistance of RC beams.

The formulation proposed by Nanni *et al.* for the NSM shear strengthening technique was applied to the tested beams of low concrete strength. In general, this formulation provided safe and acceptable estimates for the contribution of the NSM shear strengthening systems (the predicted values of the CFRP contribution for the shear resistance were 75% of the results registered experimentally).

Acknowledgements

The authors wish to acknowledge the support provided by the “Empreiteiros Casais”, Degussa, S&P® and Secil (Unibetão, Braga). The study reported in this paper forms a part of the research program supported by FCT, PTDC/ECM/73099/2006.

References

[1] ACI Committee 440, “Guide for the design and construction of externally bonded FRP systems for strengthening concrete structures”, American Concrete Institute, 118 p. (2002).

[2] *fib* - Bulletin 14, “Externally bonded FRP reinforcement for RC structures”, Technical report by Task Group 9.3 FRP (Fiber Reinforced Polymer) reinforcement for concrete structures, Féderation Internationale du Béton - *fib*, July, 130 pp. (2001).

[3] Bakis, C.E., Bank, L.C., Brown, V.L., Cosenza, E., Davalos, J.F., Lesko, J.J., Machida, A., Riskalla, S.H. and Triantafillou, T.C., “Fiber-reinforced polymer composites for construction – state-of-the-art review”, Journal of Composites for Construction, 6(2), 73-87 (2002).

[4] Bousselham A. and Chaallal O., “Shear strengthening reinforced concrete beams with fiber-reinforced polymer: assessment of influencing parameters and required research”, ACI Structural Journal, 101(2), 219-227 (2004).

[5] Bousselham, A. and Chaallal, O., “Behavior of reinforced concrete T-beams strengthened in shear with carbon fiber-reinforced polymer - an experimental study”, ACI Structural Journal, 103(3), 339-347 (2006).

[6] Jayaprakash, J., Samad, A., Abbasovich, A. and Ali, A., “Shear capacity of precracked and non-precracked reinforced concrete shear beams with externally bonded bi-directional CFRP strips”, Construction and Building Materials (2007).

[7] Mosallam, A. and Banerjee, S., “Shear enhancement of reinforced concrete beams strengthened with FRP composites laminates”, Composites: Part B, 38, 781-793 (2007).

[8] De Lorenzis, L. and Nanni, A., “Shear Strengthening of Reinforced Concrete Beams with Near-Surface Mounted Fiber-Reinforced Polymer Rods”, ACI Structural Journal, 98(1), 60-68 (2001).

[9] Carolin, A., “Carbon fibre reinforced polymers for strengthening of structural elements”, PhD thesis, Lulea University of Technology (2003).

[10] Barros, J.A.O. and Dias, S.J.E., “Shear strengthening of reinforced concrete beams with laminate strips of

CFRP", Proceedings of the International Conference Composites in Constructions - CCC2003, Cosenza, Italy, 16-19 September, 289-294 (2003).

[11] Nanni, A., Di Ludovico, M. and Parretti, R., "Shear strengthening of a PC bridge girder with NSM CFRP rectangular bars", Advances in Structural Engineering, 7(4), 97-109 (2004).

[12] El-Hacha, R. and Riskalla, S.H., "Near-surface-mounted fiber-reinforced polymer reinforcements for flexural strengthening of concrete structures", ACI Structural Journal, 101(5), 717-726 (2004).

[13] Barros, J.A.O. and Dias, S.J.E., "Near surface mounted CFRP laminates for shear strengthening of concrete beams", Journal Cement and Concrete Composites, 28(3), 276-292 (2006).

[14] Dias, S.J.E. and Barros, J.A.O., "Behaviour of RC beams shear strengthening with NSM CFRP laminates", Proceedings of the International Conference CCC2008 - Challenges for Civil Construction, 16-18 April, Portugal (2008).

[15] Dias, S.J.E. and Barros, J.A.O., "Influence of the percentage of steel stirrups in the effectiveness of the NSM laminates shear strengthening technique", Proceedings of FRPRCS-9, 9th International Symposium on Fiber Reinforced Polymer Reinforcement for Concrete Structures, 13-15 July, Australia (2009).

[16] Bianco, V., Barros, J.A.O. and Monti, G., "Three dimensional mechanical model for simulating the NSM FRP strips shear strength contribution to RC beams", Engineering Structures Journal, doi:10.1016/j.engstruct.2008.12.017 (2009).

[17] Collins, M. P., and Mitchell, D., "Prestressed Concrete Structures", Prentice-Hall, Inc., Englewood Cliffs, New Jersey (1997).

[18] EN 206-1, "Concrete - Part 1: Specification, performance, production and conformity." European standard, CEN, 69 pp. (2000).

[19] EN 10002-1, "Metallic materials - Tensile testing. Part 1: Method of test (at ambient temperature)", European Standard, CEN, Brussels, Belgium, 35 pp. (1990).

[20] ISO 527-5, "Plastics - Determination of tensile properties - Part 5: Test conditions for unidirectional fibre-reinforced plastic composites", International Organization for Standardization (ISO), Geneva, Switzerland, 9 pp. (1997).

[21] Degussa Construction Chemicals Portugal, Technical Report MBrace Resin 220, May (2003).

[22] ACI Committee 318, "Building code requirements for structural concrete and commentary", American Concrete Institute, Reported by ACI Committee 118 (1999).

FIGURES AND TABLES

List of Figures:

Fig. 1 - Tested beams: geometry, steel reinforcements applied in all beams (dimensions in mm)

Fig. 2 - Localization of the steel stirrups (continuous line) and CFRP laminates (dashed line) in the tested beams (dimensions in mm)

Fig. 3 - Positions of the strain gauges in the monitored laminates and stirrups

Fig. 4 - Force *vs* deflection at the loaded-section and $\Delta F/F^{2S\text{-}R}$ *vs* deflection at the loaded-section for the beams with ρ_{sw} = 0.10% strengthened with the lower (a) and higher (b) percentage of CFRP shear strengthening

Fig. 5 - Force *vs* deflection at the loaded-section and $\Delta F/F^{4S\text{-}R}$ *vs* deflection at the loaded-section for the beams with ρ_{sw} = 0.17% strengthened with the lower (a) and higher (b) percentage of CFRP shear strengthening

Fig. 6 - Influence of the percentage of existing steel stirrups in the effectiveness of the NSM shear strengthening technique using CFRP laminates

Fig. 7 - Details of the failure zones of the tested beams

Fig. 8 - Influence of CFRP percentage on failure modes

Fig. 9 - Strains in the monitored laminates of the 4S-4LI45 beam

Fig. 10 - Strains in the monitored steel stirrup of the 4S-4LI45 beam

Fig. 11 - Influence of the concrete strength in the effectiveness of the NSM shear strengthening technique using CFRP laminates (left column: f_{cm} = 39.7 MPa, right column: f_{cm} = 18.7 MPa)

Fig. 12 - Graphical representation of variables used in the formulation by Nanni *et al.* (for this example $\sum_i L_i = L_2 + L_3 + L_4$)

Fig. 13 - Graphical representation of l_{max}

List of Tables:

Table 1 - CFRP shear strengthening configurations of the tested beams

Table 2 - Values of the properties of intervening materials

Table 3 - Relevant results in terms of the load capacity up to beam’s failure

Table 4 - Strain variation in monitored laminates and steel stirrup of 4S-4LI45 beam (strain values in %)

Table 5 - Influence of the concrete strength in the effectiveness of the NSM shear strengthening technique with CFRP laminates

Table 6 - Analytical *vs* experimental results for the tested beams with NSM CFRP laminates

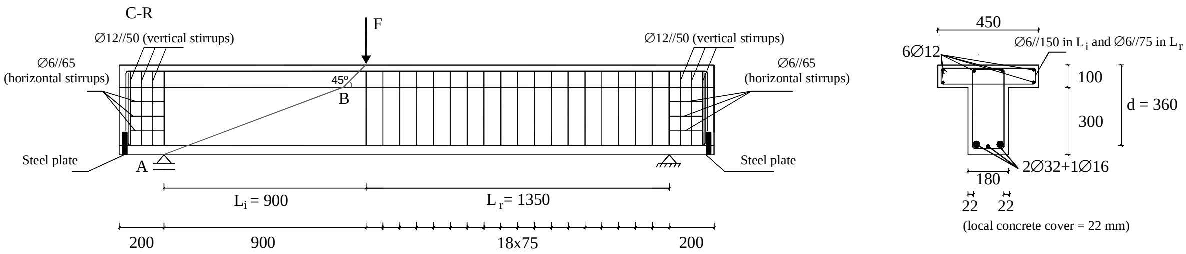

Fig. 1 - Tested beams: geometry, steel reinforcements applied in all beams (dimensions in mm)

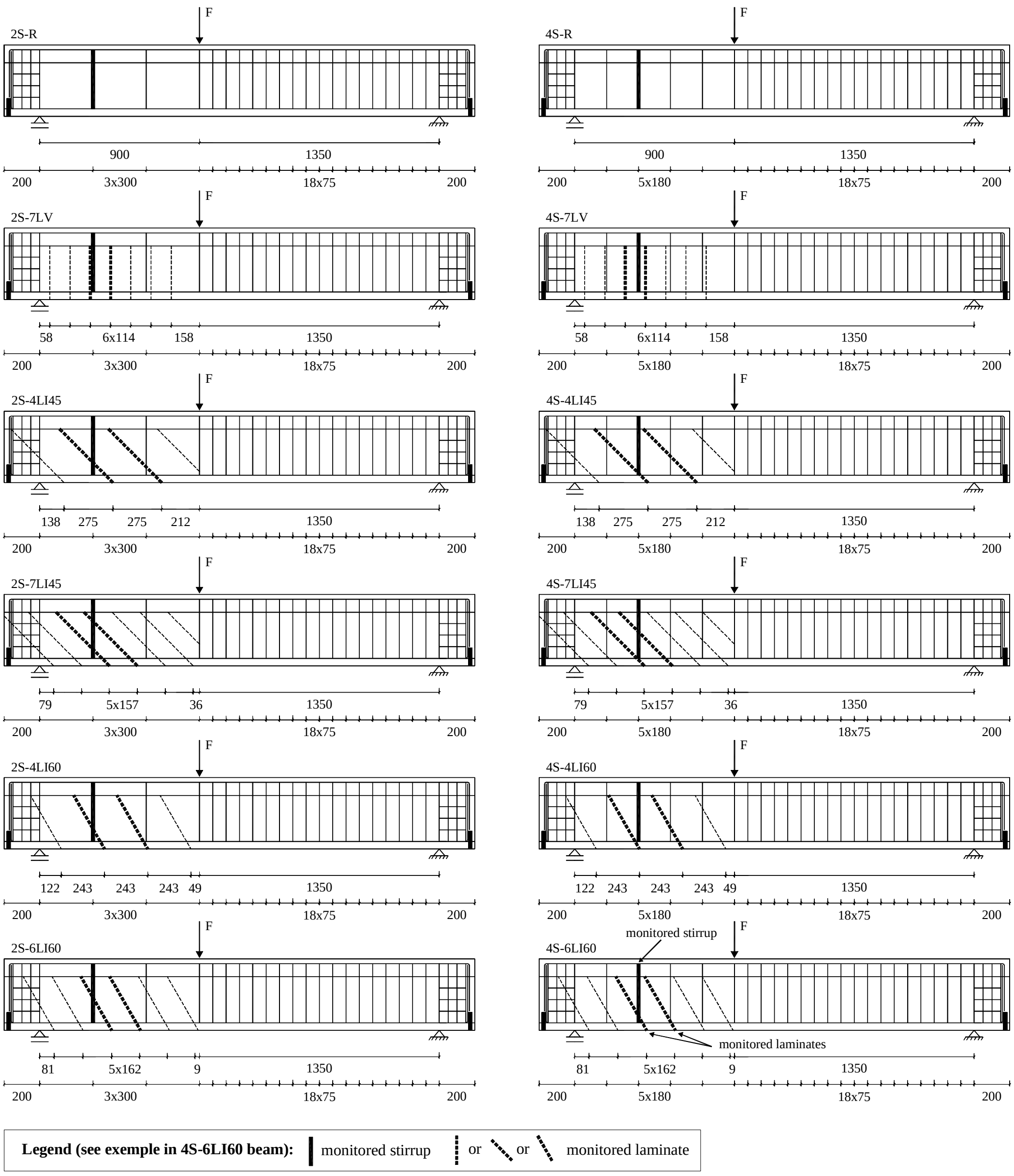

Fig. 2 - Localization of the steel stirrups (continuous line) and CFRP laminates (dashed line) in the tested beams (dimensions in mm)

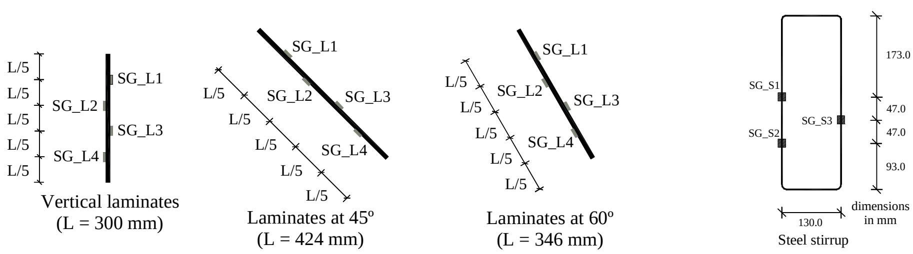

Fig. 3 - Positions of the strain gauges in the monitored laminates and stirrups

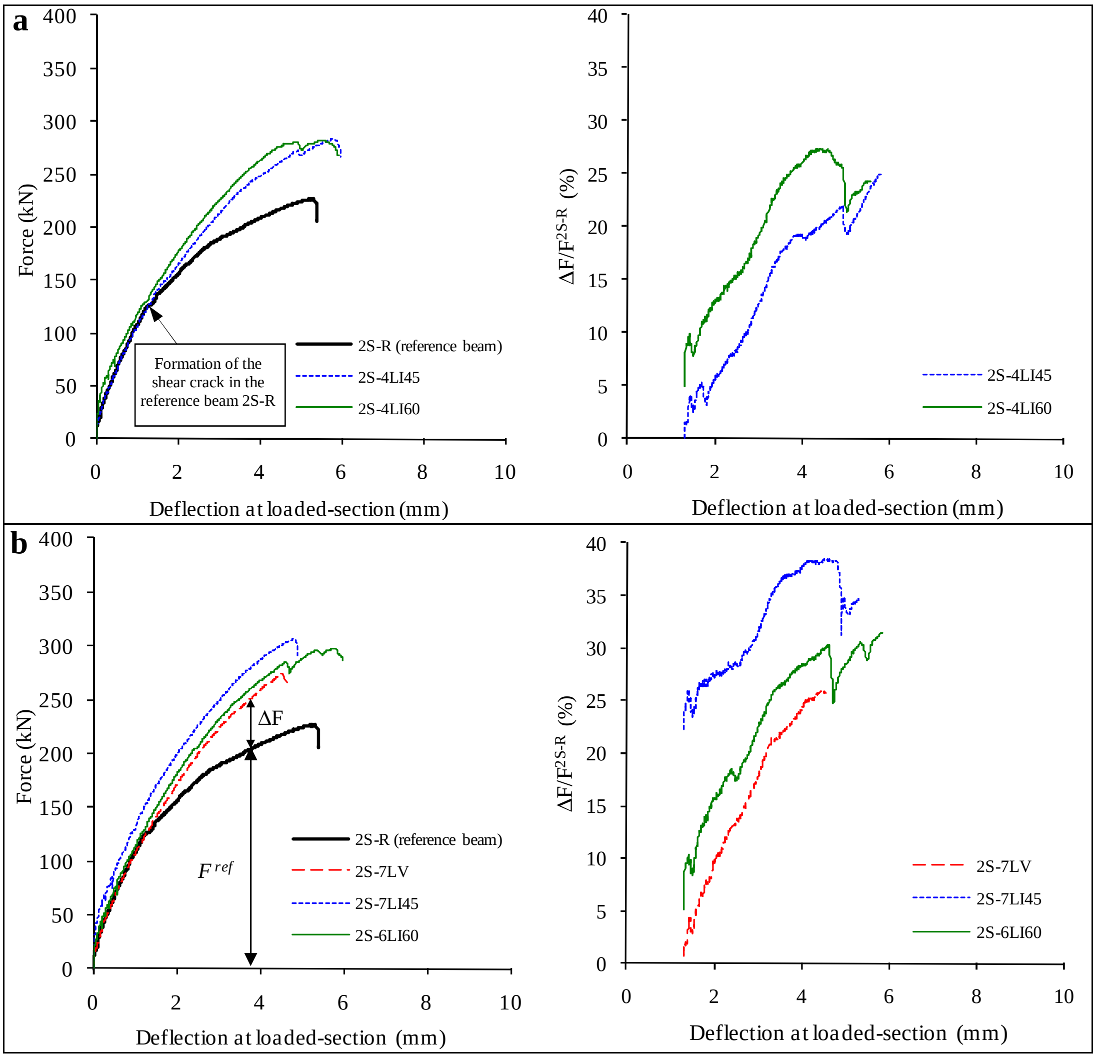

Fig. 4 - Force *vs* deflection at the loaded-section and $\Delta F/F^{2S\text{-}R}$ *vs* deflection at the loaded-section for the beams with ρ_{sw} = 0.10% strengthened with the lower (a) and higher (b) percentage of CFRP shear strengthening

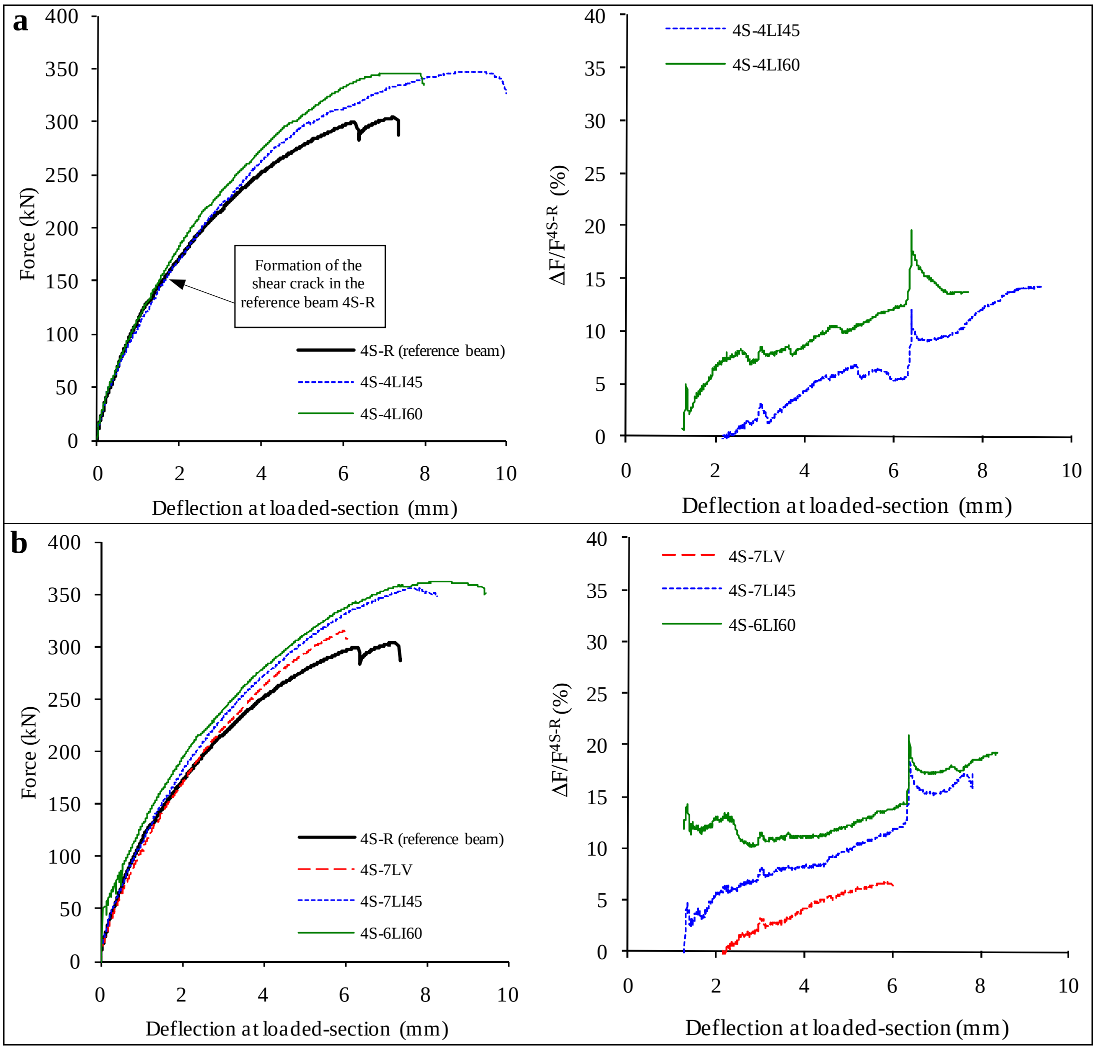

Fig. 5 - Force *vs* deflection at the loaded-section and $\Delta F/F^{4S-R}$ *vs* deflection at the loaded-section for the beams with ρ_{sw} = 0.17% strengthened with the lower (a) and higher (b) percentage of CFRP shear strengthening

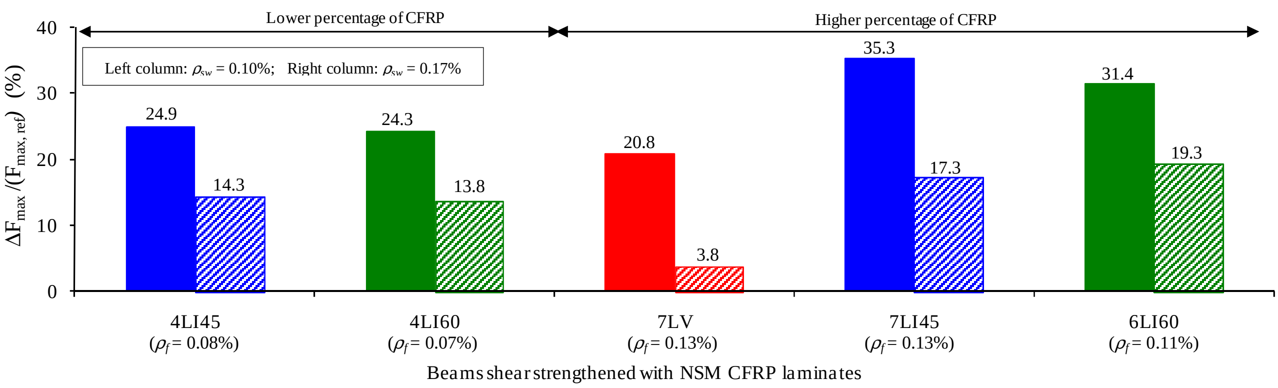

Fig. 6 - Influence of the percentage of existing steel stirrups in the effectiveness of the NSM shear strengthening technique using CFRP laminates

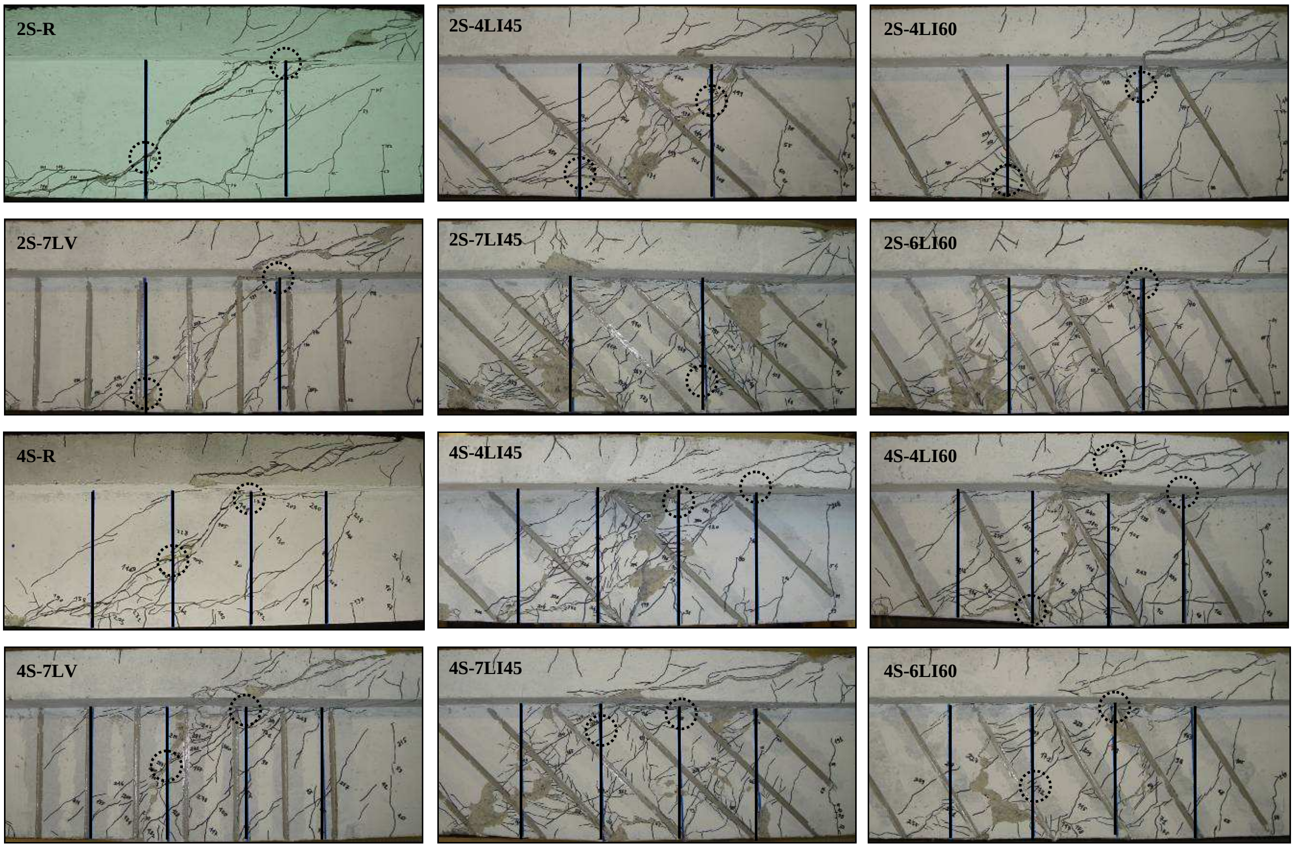

Fig. 7 - Details of the failure zones of the tested beams

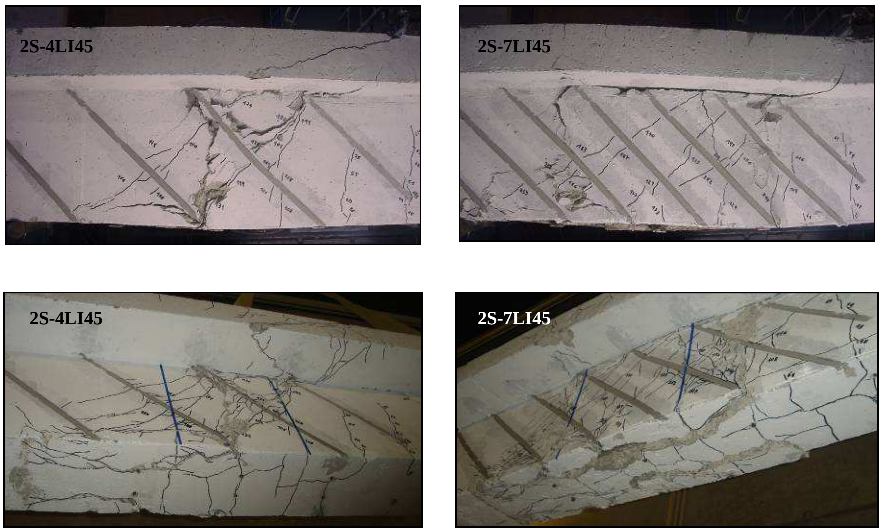

Fig. 8 - Influence of CFRP percentage on failure modes

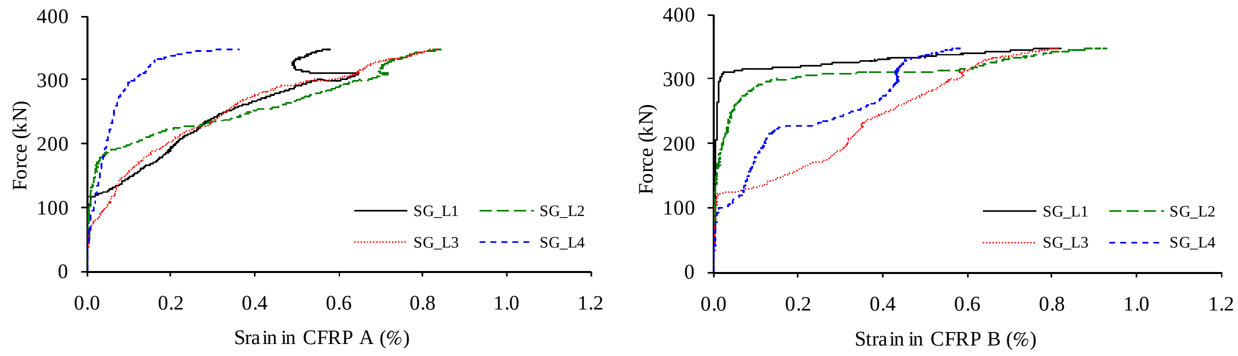

Fig. 9 - Strains in the monitored laminates of the 4S-4LI45 beam

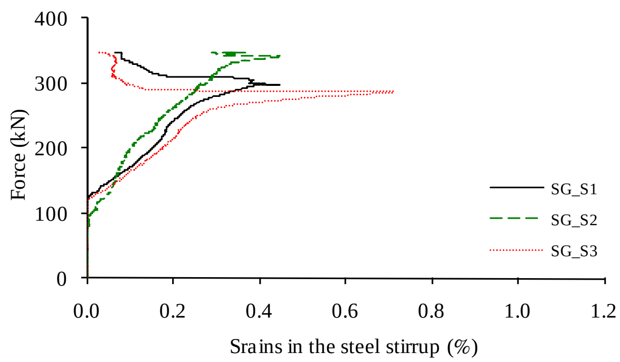

Fig. 10 - Strains in the monitored steel stirrup of the 4S-4LI45 beam

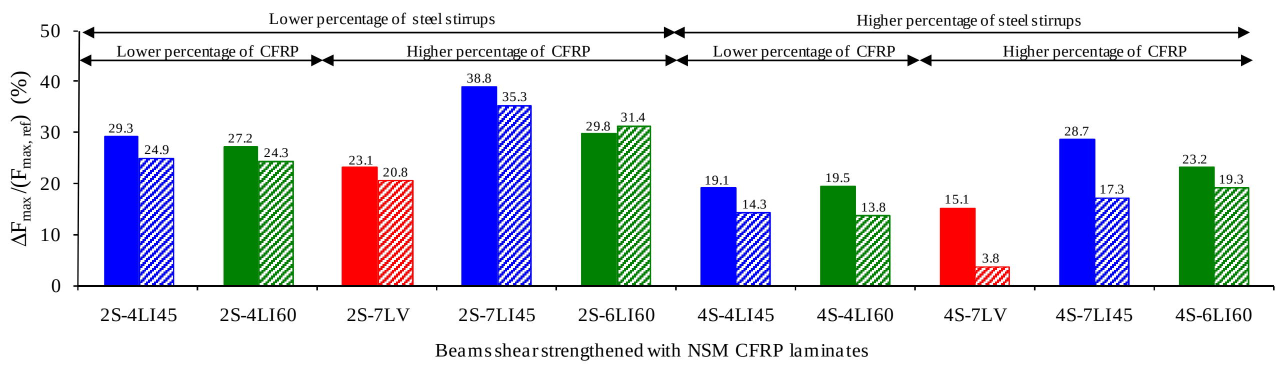

Fig. 11 - Influence of the concrete strength in the effectiveness of the NSM shear strengthening technique using CFRP laminates (left column: f_{cm} = 39.7 MPa, right column: f_{cm} = 18.6 MPa)

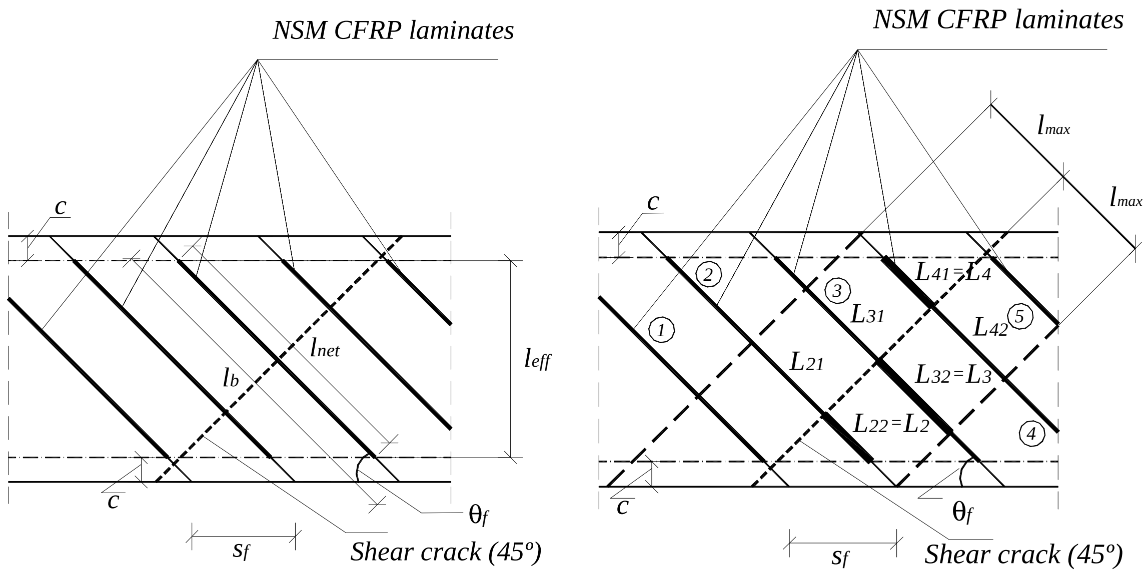

Fig. 12 - Graphical representation of variables used in the formulation by Nanni *et al.* (for this example $\sum_i L_i = L_2 + L_3 + L_4$)

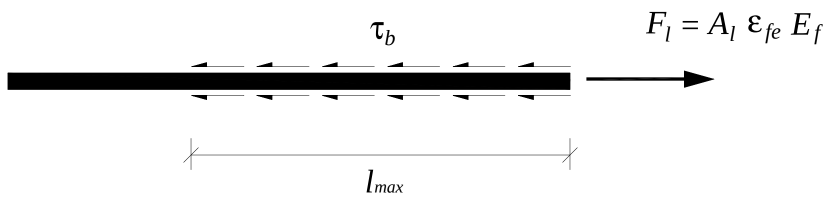

Fig. 13 - Graphical representation of l_{max}

Table 1 - CFRP shear strengthening configurations of the tested beams

Number of laminates	Angle [θ_f] (º) [a]	CFRP spacing [s_f] (mm)	CFRP percentage [ρ_f] (%) [b]	Percentage of steel stirrups [ρ_{sw}]	
				0.10% [c]	0.17% [d]
2×7	90	114	0.13	2S-7LV	4S-7LV
2×4	45	275	0.08	2S-4LI45	4S-4LI45
2×7	45	157	0.13	2S-7LI45	4S-7LI45
2×4	60	243	0.07	2S-4LI60	4S-4LI60
2×6	60	162	0.11	2S-6LI60	4S-6LI60

[a] Angle between the CFRP fiber direction and the beam axis; [b] The CFRP percentage was obtained from $\rho_f = (2 a_f b_f)/(b_w s_f \sin\theta_f)$ being a_f = 1.4 mm and b_f = 9.5 mm the dimensions of the laminate cross section, and b_w = 180 mm is the beam web width; [c] 2S-R is the reference beam without CFRP (Fig. 2); [d] 4S-R is the reference beam without CFRP (Fig. 2).

Table 2 - Values of the properties of intervening materials

Concrete	Compressive strength [f_{cm}] (MPa)				
	15.9 MPa (at 28 days)		18.6 MPa (at 51 days - age of beam tests)		
Steel	Diameter (mm)	ϕ6	ϕ12	ϕ16	ϕ32
	Yield stress [f_{sym}] (MPa)	539	453	429	734
	Tensile strength [f_{sum}] (MPa)	595	581	563	885
CFRP Laminates	Tensile strength [f_{fum}] (MPa)	Young's Modulus [E_{fm}] (GPa)		Maximum strain [ε_{fu}] (%)	
	2847.9	174.3		1.63	

Table 3 - Relevant results in terms of the load capacity up to beam's failure

Beam designation	$(\Delta F/F^{ref})_{max}$ (%)	$u_{(\Delta F/F^{ref})_{max}}$ (mm)	F_{max} (kN)	$\Delta F_{max}/F_{max}^{ref}$ (%)	$u_{F_{max}}$ (mm)	ε_{CFRP}^{max} (%)	$(\varepsilon_{CFRP}^{max})_{med}$ (%)
C-R	-	-	147.0	-	3.44	-	-
2S-R	-	-	226.5	-	5.29	-	-
2S-7LV	26.1	4.48	273.7	20.8	4.55	0.57	0.49
2S-4LI45	24.9	5.79	283.0	24.9	5.79	0.94	0.72
2S-7LI45	38.5	4.50	306.5	35.3	4.79	0.65	0.53
2S-4LI60	27.4	4.45	281.6	24.3	5.57	0.70	0.69
2S-6LI60	31.4	5.84	297.7	31.4	5.84	0.65	0.59
4S-R	-	-	303.8	-	7.20	-	-
4S-7LV	6.7	5.88	315.2	3.8	5.98	0.71	0.41
4S-4LI45	14.3	9.28	347.2	14.3	9.28	0.93	0.88
4S-7LI45	19.3	6.38	356.4	17.3	7.83	0.71	0.60
4S-4LI60	19.6	6.38	345.6	13.8	7.67	0.78	0.75
4S-6LI60	20.9	6.38	362.3	19.3	8.36	0.54	0.52

Table 4 - Strain variation in monitored laminates and steel stirrup of 4S-4LI45 beam (strain values in %)

<table>
<tr><td colspan="3">Description</td><td colspan="6" rowspan="2">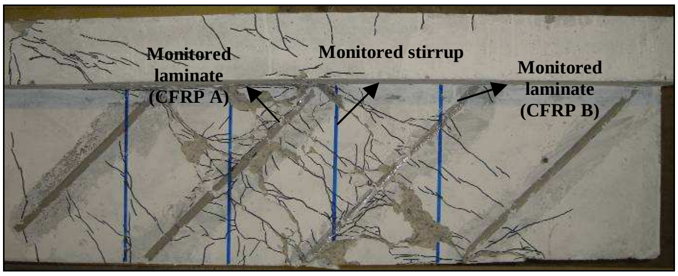
</td></tr>
<tr><td colspan="3">The beam failed by debonding of the CFRP A at F_{max} = 347.2 kN.</td></tr>
<tr><td rowspan="5">CFRP A</td><td rowspan="5">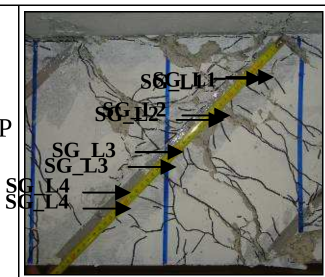
</td><td>SG_L</td><td>F =150 kN</td><td>F =200 kN</td><td>F =250 kN</td><td>F =300 kN</td><td>F =340 kN</td><td>F =347.2 kN</td></tr>
<tr><td>1</td><td>0.11</td><td>0.21</td><td>0.33</td><td>0.61</td><td>0.53</td><td>0.58</td></tr>
<tr><td>2</td><td>0.02</td><td>0.11</td><td>0.39</td><td>0.68</td><td>0.78</td><td>0.84</td></tr>
<tr><td>3</td><td>0.09</td><td>0.20</td><td>0.33</td><td>0.58</td><td>0.78</td><td>0.84</td></tr>
<tr><td>4</td><td>0.03</td><td>0.05</td><td>0.07</td><td>0.11</td><td>0.22</td><td>0.36</td></tr>
<tr><td rowspan="5">CFRP B</td><td rowspan="5">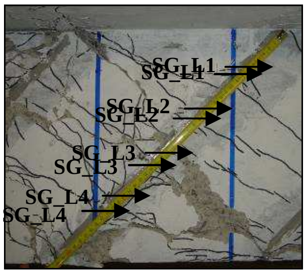
</td><td>SG_L</td><td>F =150 kN</td><td>F =200 kN</td><td>F =250 kN</td><td>F =300 kN</td><td>F =340 kN</td><td>F =347.2 kN</td></tr>
<tr><td>1</td><td>0.00</td><td>0.00</td><td>0.01</td><td>0.02</td><td>0.62</td><td>0.82</td></tr>
<tr><td>2</td><td>0.10</td><td>0.02</td><td>0.05</td><td>0.18</td><td>0.79</td><td>0.93</td></tr>
<tr><td>3</td><td>0.17</td><td>0.32</td><td>0.42</td><td>0.58</td><td>0.74</td><td>0.81</td></tr>
<tr><td>4</td><td>0.08</td><td>0.12</td><td>0.33</td><td>0.43</td><td>0.52</td><td>0.58</td></tr>
<tr><td rowspan="4">Steel stirrup</td><td rowspan="4">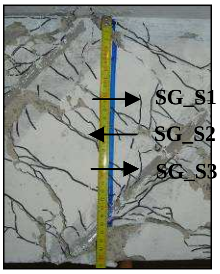
</td><td>SG_S</td><td>F =150 kN</td><td>F =200 kN</td><td>F =250 kN</td><td>F =300 kN</td><td>F =340 kN</td><td>F =347.2 kN</td></tr>
<tr><td>1[a]</td><td>0.06 (0.14)</td><td>0.15 (0.23)</td><td>0.22 (0.27)</td><td>0.38 (0.35)</td><td>0.08</td><td>0.06</td></tr>
<tr><td>2[a]</td><td>0.07 (0.19)</td><td>0.10 (0.45)</td><td>0.18 (0.68)</td><td>0.28 (0.84)</td><td>0.43</td><td>0.37</td></tr>
<tr><td>3[b]</td><td>0.08</td><td>0.18</td><td>0.26</td><td>0.09</td><td>0.06</td><td>0.03</td></tr>
</table>

Note: To localize the SGs applied in the two arms of the steel stirrup, the arrow which points to the left indicates the SG applied in the arm at the opposite side of the one represented in the Figure. [a] Values in brackets are those recorded in the 4S-R beam at F_{max}=303.8 kN. [b] This SG did not work in the reference beam 4S-R.

Table 5 - Influence of the concrete strength in the effectiveness of the NSM shear strengthening technique with CFRP laminates

CFRP		f_{cm} = 39.7 MPa				f_{cm} = 18.6 MPa			
Percentage (%)	Angle (º)	Beams	$\Delta F_{max} / F_{max}^{ref}$ (%)	$u_{F_{max}} / u_{F\,max}^{ref}$ (%)	ε_{CFRP}^{max} (%) [a]	Beams	$\Delta F_{max} / F_{max}^{ref}$ (%)	$u_{F_{max}} / u_{F\,max}^{ref}$ (%) [b]	ε_{CFRP}^{max} (%)
0.13	90	2S-7LV	23.1	21.9	0.77	2S-7LV	20.8	-14.0	0.57
0.08	45	2S-4LI45	29.3	9.7	1.08	2S-4LI45	24.9	9.5	0.94
0.07	60	2S-4LI60	27.2	17.3	0.99	2S-4LI60	24.3	5.3	0.70
0.13	45	2S-7LI45	38.8	34.9	0.85	2S-7LI45	35.3	-9.5	0.65
0.11	60	2S-6LI60	29.8	33.8	0.99	2S-6LI60	31.4	10.4	0.65
0.13	90	4S-7LV	15.1	56.0	0.91	4S-7LV	3.8	-16.9	0.71
0.08	45	4S-4LI45	19.1	26.9	0.79	4S-4LI45	14.3	28.9	0.93
0.07	60	4S-4LI60	19.5	10.6	0.94	4S-4LI60	13.8	6.5	0.78
0.13	45	4S-7LI45	28.7	32.2	0.82	4S-7LI45	17.3	8.8	0.71
0.11	60	4S-6LI60	23.2	17.0	0.87	4S-6LI60	19.3	16.1	0.54

[a] For the beams 4S-7LV, 4S-4LI45, 4S-4LI60, 4S-7LI45 and 4S-6LI60 only one laminate has been monitored. [a] In the beams with negative value the deflection at the loaded section for the maximum load was lower than that of observed in the reference beam.

Table 6 - Analytical *vs* experimental results for the tested beams with NSM CFRP laminates

Beam designation	Experimental	Formulation by Nanni *et al.* [11]	
	$V_f^{exp.}$ (kN)	V_{fd}^{ana} (kN)	$V_f^{exp.} / V_{fd}^{ana}$
2S-7LV	28.3	29.9	0.95
2S-4LI45	33.9	14.0	2.42
2S-7LI45	48.0	34.3	1.40
2S-4LI60	33.1	17.1	1.94
2S-6LI60	42.7	34.2	1.25
4S-7LV	6.8	29.9	0.23
4S-4LI45	26.0	14.0	1.86
4S-7LI45	31.6	34.3	0.92
4S-4LI60	25.1	17.1	1.47
4S-6LI60	35.1	34.2	1.03